GEOPHYSICAL RESEARCH LETTERS, VOL. 34, L05301, doi:10.1029/2006GL028980, 2007

Stress and fluid transfer in a fault zone due to overpressures in the seismogenic crust

Frédéric Cappa,[1] Yves Guglielmi,[2] and Jean Virieux[2]

Received 13 December 2006; revised 27 January 2007; accepted 1 February 2007; published 1 March 2007.

[1] Stress and fluid transfers were analyzed on the surface of a 30 m thick dextral strike-slip fault zone subjected to an overpressure of 63 kPa. Pressure-strain measurements taken during the pressurization indicated a strain state primarily controlled by the hydromechanical behavior of permeable fractures, and then, by the fluid diffusion in the matrix. Using THM modeling, we simulated an extension of these hydromechanical effects to a 25 km depth in the seismogenic crust, applying a lithostatic pressure at the base of the fault. The simulations indicate that a significant strain in the damage zone greater than that in the protolith, along with the differences in hydraulic diffusivity between the damage zone and protolith, may induce high static stress and fluid accumulations in the core. Under this stress, this core is projected to exhibit deformity—as much as a 12 m shear slip distributed over a 175 m long active zone. **Citation:** Cappa, F., Y. Guglielmi, and J. Virieux (2007), Stress and fluid transfer in a fault zone due to overpressures in the seismogenic crust, *Geophys. Res. Lett.*, *34*, L05301, doi:10.1029/2006GL028980.

1. Introduction

[2] Several seismic tomographic studies of tectonically active zones (seismogenic zones) around the world have identified structures at seismogenic depths with velocities that could be result from high-fluid pressures [*Zhao et al.*, 1996; *Husen et al.*, 2000]. Such fluid pressures, which may induce seismicity in the seismogenic crust by reducing the strength of fault zones (the most active area within a seismogenic zone), may also potentially control the nucleation and recurrence of earthquake ruptures [*Sibson and Rowland*, 2003]. However, characterization of the coupling among stress, fluids and structural thermo-hydro-mechanical (THM) properties in seismogenetic zones (and notably near fault zones), is difficult—and requires field investigations, laboratory experiments and numerical simulations to be properly carried out.

[3] Fault zones in themselves contain complex structures—generally a fault core and a damage zone—that have distinct mechanical and permeability properties [*Gudmundsson*, 1999; *Wibberley and Shimamoto*, 2003]. The fault core is a low-permeable zone with small inter-granular porosity, whereas the damage zone is a more permeable zone with a macroscopic fracture network. Depending on host rock lithology and fault dimensions and movement, the permeability of the fault zone may vary drastically, making the zone act either as a barrier or as a conduit for fluid flows [*Caine et al.*, 1996]. Moreover, the seismogenic permeability of the fault zone changes during shear slip and the sudden stress reduction associated with earthquakes [*Uehara and Shimamoto*, 2004]. Field data and models indicate that the core/damage zone contact often ruptures during earthquakes. Both the core and damage zones grow in thickness with increasing displacement, and fractures that open allow fluid flow in those zones [*Gudmundsson*, 2004]. Before and after ruptures, fluid flow can occur in the damage zone, whereas the core may act as a barrier to flow, depending on the trend of the fault zone in relation to that of the flow [*Gudmundsson*, 2000, 2001]. Thus, during inter-seismic periods, coupled poroelastic processes can cause pressure and strain accumulations in the damage zone—which may play a major role in fault rupture processes and stress release in the crust.

[4] Such poroelastic stress transfer induced by fluid flow is generally difficult to characterize at seismogenic depths, either by seismic wave measurements or borehole studies. Near the free surface, however, detailed structural analyses of fault zones are possible and can be combined with laboratory permeability measurements on samples.

[5] In our research, we first investigated, in situ, the hydromechanical behavior in the outcropping portion of a regional fault zone in carbonate rock at the Coaraze Laboratory in France [*Guglielmi*, 1998]. At this medium-scale site, where the piezometric level can be artificially controlled, various measurements were taken, with coupled fluid pressure and strain sensors localized on several fault-related fractures (subfaults) and matrix zones at depth. In this paper, we analyse these data, giving special attention to the poroelastic stress transfer in the fault zone. Assuming the same rheological behavior at greater depth, we can then infer the hydromechanical conditions in a similar fault at seismographic depths, using coupled THM simulations to develop an enhanced model of poroelastic strain accumulation in a fault zone during inter-seismic periods.

2. Fault Zone Structure

[6] The Coaraze research site, the studied fault zone, corresponds to a subvertical dextral strike-slip fault trending N140°E, located 20 km east of Nice, at the junction between the Southern Alps and the Ligurian Basin, a moderately active seismic area for Western Europe (Figure 1a). Some segments of the fault show earthquake seismic activity at magnitudes of up to 6.0, at depths of 2 to 6 km [*Larroque et al.*, 2001].

[7] Fortunately, the outcropping portion of the fault zone has been accurately mapped at this site (Figure 1b). The

[1] Earth Sciences Division, Lawrence Berkeley National Laboratory, Berkeley, California, USA.
[2] Géosciences Azur, Centre National de la Recherche Scientifique-Insitut de Recherche pour le Développement-Université Nice Sophia Antipolis-Université Pierre and Marie Curie, Sophia-Antipolis, France.

0094-8276/07/2006GL028980$05.00

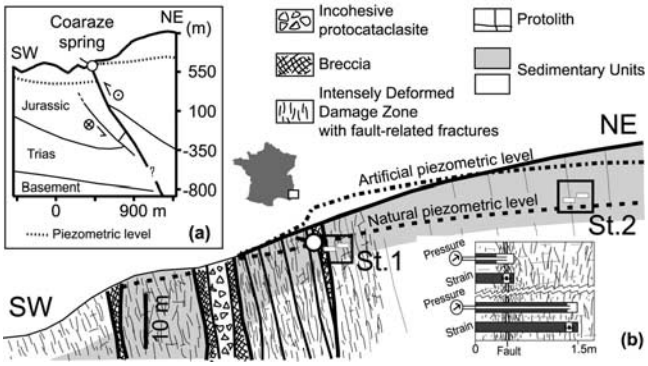

Figure 1. (a) General and (b) close-up sections of the fault zone structure at the Coaraze site.

total horizontal displacement of the fault is of 30–40 m and is localized on a set of subparallel slip surfaces. Discontinuous fault cores made up of breccia and protocataclasite of 0–5 m wide occur along some of the surfaces. Cataclasite fragments are millimetres-to-centimetres in size, and they are surrounded by finer calcareous matrix with a varying amount of calcite cement. Damage zones are characterized by centimetres-long subfaults, with an average spacing of 0.07 m. Inherited, strongly deformed bedding planes and styloliths are observed, with an average spacing of 0.2 m. The centimetres-long offsets could be caused by some decametric subfaults, with an average spacing of 2 m in the damage zone. This zone gradually fades about 5 to 10 m outward into the intact protolith, which is a typical fractured limestone containing inherited fractures and bedding planes, with average spacing of 5 and 0.2 m, respectively.

[8] A spring with an average annual yield of 10 l/s outflows close to the fault core (Figure 1). This spring drains the reservoir (located in a Cretaceous unit), the fault core acting as an impervious boundary because the aquifer piezometric level shifts more than 50 m between the two walls of the fault (Figure 1b). A water gate is set on the spring, and the topographic surface upward the fault is clogged with concrete. By opening and closing the water gate, the piezometric level in the hanging wall of the fault can be artificially varied (Figure 1b). The fault is instrumented for detailed hydromechanical measurements during fluid pressure changes [*Cappa et al.*, 2005].

[9] We set up an experimental device at this site to monitor strain and pressure changes into the damage zone and the protolith (Figure 1b, respectively St.1 and St.2). Changes in fluid pressures and strains were simultaneously monitored on single subfaults and in the rock matrix, by coupling several 15 cm long vibrating-wire extensometers with pressure gauges. At a so-called coupled pressure-strain measuring point, these two sensors were installed in two small parallel boreholes (Ø = 45 mm) spaced about 0.3 m. Fluid pressure is measured within an accuracy of 0.5 kPa, and strain within an accuracy of 0.5 μm/m.

3. Evidence of Coupled Strain and Fluid Transfer in a Fault Zone

[10] By closing the gate, we applied a pressure increase of 63 kPa for 1 hour in the fault zone. During the hydraulic loading, the pressure increased to 63 kPa in the damage zone and to 40 kPa in the protolith, 30 m upstream the gate (St.1 and St.2 in Figure 2). Pressure increased during 12 mn in the main subfaults of the damage zone and in the connected inherited fractures of the protolith. Pressure stabilization began after 12 mn transient flow, and the maximum pressure (63 kPa) reaches a steady state 60 mn after water gate closure. In the rock matrix, the pressure rise is small (20 kPa), much slower than the pressure rise in the subfaults. Using pulse tests, *Cappa et al.* [2005] have shown that fluid flow in the fault zone is controlled by dual-permeability behavior, with highly permeable subfaults ($k = 10^{-12}$ m^2) bounding low-permeable rock-matrix blocks ($k = 10^{-18}$ m^2). Coupled measurements of pressure and fault-normal mechanical displacement indicate a direct hydromechanical coupling in the main subfaults and in the inherited fractures, where a pressure increase is directly accompanied by subfault opening (Figure 2). Displacement normal to the subfault stabilizes when pressure stops varying, and reaches values of 0.8 to 1.2 $\times$ 10^{-6} m. The normal displacement-versus-pressure curves show very different shapes—highly nonlinear in the fault damage zone and almost linear in the protolith.

[11] Hydromechanical coupling within the rock matrix is more complex than subfaults. In the damage zone (St.1, Figure 2), the normal displacement increases independent of pressure between 0 and 12 mn, and is caused by the matrix poroelastic response to the main subfault opening. Then, normal displacement follows the slow pressure variation in the matrix, reaching a value of 1 $\times$ 10^{-6} m after 1 hour of hydraulic loading. In the protolith, no displacement change is observed (St.2, Figure 2).

[12] Strong but very different coupling between permeability and strain in the damage zone and the protolith has been identified when interpreting strain data. The damage zone behaves like a double-permeability, highly deformable media, with connected, highly permeable, not-so-rigid subfaults, and a low-permeable, low-rigidity matrix affected by a concentration of small fractures. Fluid pressure in the protolith follows the same conceptual scheme, but the

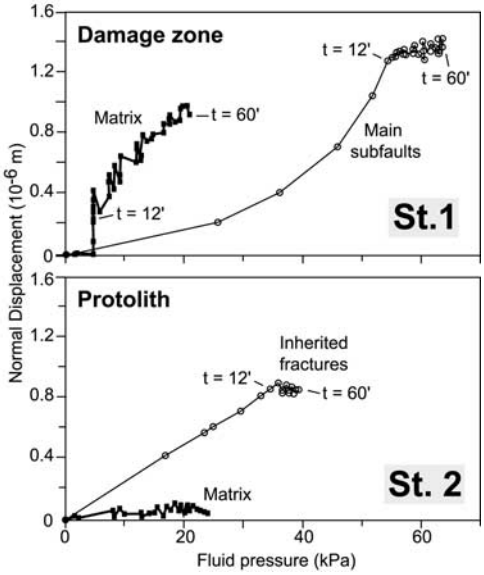

Figure 2. Hydromechanical data at St.1 and St.2.

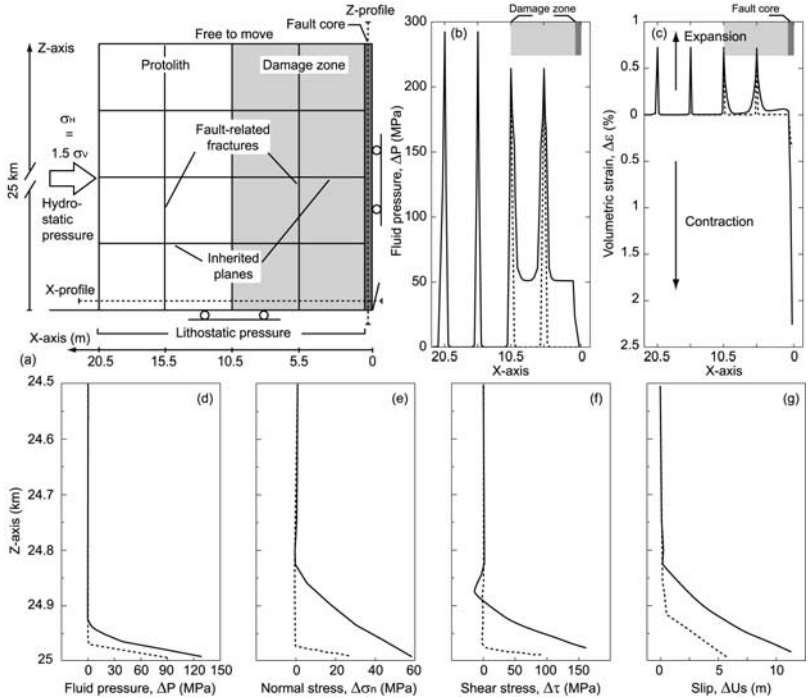

Figure 3. (a) Close-up view of initial conditions of the 3D fault zone model. Model results when pressures and strains are steady-state: horizontal profiles of changes in (b) fluid pressure, and (c) volumetric strain at 50 m above the basal boundaries (X-profile); vertical profiles of changes in (d) fluid pressure, (e) total normal stress, (f) total shear stress, and (g) shear slip along the fault core (Z-profile). (Solid lines, model with a damage zone; dashed line, model without damage zone).

hydromechanical coupling appears very different, mainly because the matrix, being less fractured, is more rigid than in the damage zone. Thus, pore pressure diffusion can grow farther outward in the protolith, with contrasted hydromechanical effects—the damage zone being more permeable and deformable than the protolith because of its high concentration of connected subfaults.

4. Thermo-Hydro-Mechanical (THM) Model

[13] To investigate fluid-strain coupling on stress accumulation in a vertical fault zone at seismogenic depths, we developed a finite-difference THM model, assuming the same rigidity-permeability contrasts—as those observed at shallow depth—in the protolith, the damage zone–core system relationship is still presumed valid at greater depth. The generic THM model enables a detailed evaluation of the sensitivity of the stress state to fluid-strain coupling. In this model, pressurization is applied down to a 25 km depth at the base of the seismogenic crust to simulate the effects of high lithostatic pressure. Two models are compared, one without a damage zone and one with an intensely deformed damage zone. In these models, we further assume that the pressure diffuses from the deep lithostatically overpressurized zones to shallow ones at hydrostatic fluid pressure. Potential overpressurization sources at such depths may be initiated by accumulation of seawater, meteoric water, CO_2 degassing, or minerals dehydration from the mantle [*Miller et al.*, 2004].

[14] Figure 3a introduces the model geometry of the vertical fault zone in a 3D elastic medium, assuming a symmetrical axis at the right side. The model extends vertically to 25 km, and horizontally far enough from the pressurized zone. Model results are analyzed with a special attention to the area near the fault zone, which is distinctly discretized as a 0.5 m thick core embedded in a 10 m thick damage zone; and protolith, discretized as having 0.05 m thick main subfaults and inherited planes. The model is fully saturated with water in the liquid phase; the Skempton's coefficient is close to 1. Fault zone properties (Table 1) are set consistent with temperature and pressure conditions at depth; in other words, rock physics parameters are defined according to in situ stress as well as temperature and pressure conditions. For the flow problem, the distribution of initial permeability (k) and porosity (ϕ) is a function of the effective mean stress (σ'_M) as described by *Davies and Davies* [1999]:

$$\phi = (\phi_0 - \phi_r)\exp\left(-5.10^{-8} \cdot \sigma'_M\right) + \phi_r \tag{1}$$

$$k = k_0 \exp\left[22.2\left(\frac{\phi}{\phi_0} - 1\right)\right] \tag{2}$$

where ϕ_0 is porosity at zero stress, ϕ_r is residual porosity at high stress, and k_0 is the zero stress permeability. Fractured rock between major discontinuities was treated as equivalent continua reflecting fracture density and properties. Owing to model symmetry, impervious and no-displacement conditions were set normal to the right and bottom boundaries, whereas stress and fluid pressure were set to others boundaries (Figure 3a). Temperature is assumed to follow

Table 1. Model Parameters Inferred From In Situ Tests Performed by *Cappa et al.* [2005]

Model Parameters	Fault Core	Fault-Related Fractures	Inherited Planes	Damage Zone With Equivalent Properties	Rock Matrix in the Protolith
Bulk modulus, K, GPa	0.03	1.98	23.81	2.78	53.97
Shear modulus, G, GPa	0.02	0.97	11.23	1.36	26.39
Cohesion, c, kPa	1	-	-	-	-
Friction coefficient, μ_s	0.6	-	-	-	-
Dilation angle, ψ, deg.	20	-	-	-	-
Zero stress permeability, k_o, m^2	1×10^{-19}	1×10^{-8}	1×10^{-12}	1×10^{-13}	1×10^{-15}
Zero stress porosity, ϕ_o	0.01	0.5	0.5	0.5	0.05
Residual porosity, ϕ_r	0.005	0.4	0.4	0.4	0.04
Biot's coefficient, α	1	1	1	1	1
Skempton's coefficient, B	0.9	0.9	0.9	0.9	0.9
Thermal expansion, T_e, 1/°C	1×10^{-6}	-	-	8.2×10^{-6}	8.2×10^{-6}

a constant geothermal gradient with depth ($\nabla T = 25°C/km$). An in situ compressive stress regime was assumed with $\sigma_H = 1.5 \times \sigma_V$.

[15] After computing the initial state, we applied a spontaneous pressurization corresponding to the lithostatic pressure at 25 km depth ($P_l = 0.75$ GPa) at the base of both the damage zone and the protolith. In the core, shear slip occurs when the shear stress acting in the fault plane exceeds its shear strength, approximated by a Coulomb criterion:

$$\tau_{slip} = c + \mu_s(\sigma_n - \alpha P) \quad (3)$$

where τ_{slip} is the critical shear stress for slip occurrence, c is cohesion, μ_s is the static friction coefficient, σ_n is normal stress, α is Biot's coefficient, and P is fluid pressure. For the adjacent zones, a thermoporoelastic behavior was assumed. Rock permeability and porosity vary as a function of the volumetric strains induced by the pressurization. The computation is in the low-frequency domain, with fluid and solid motion in phase.

[16] Model results indicate that pore pressures vary from the very outset of the simulation run in the most permeable subfaults within the damage zone and protolith, followed by slow, laterally diffusive leakage from those subfaults to the neighboring rock matrix. Outside of the damage zone, a lateral fluid penetration of about 0.5 m occurs, whereas within the damage zone, fluid pressure increases to about 50 MPa in the matrix, an increase resulting from both the basal overpressure at 25 km depth and diffusion from the subfaults (Figure 3b). Inside the fault core, pore pressure increases to 90 MPa near the pressurization source as a result of diffusion from the surrounding matrix outside of the damage zone. Fluid pressure is greater and penetrates farther into the core when the damage zone is simulated (Figure 3d).

[17] The difference in the two models' behavior is linked both to the contrast in hydraulic diffusivity among fault zone elements and to fluid diffusion in the damage zone. The fluid pressure rise induces poroelastic stressing in the damage zone, marked by weak overpressure subfaults, with a lowered effective stress and an increased volumetric strain of about 0.7% resulting in an expansion (Figure 3c). In the damage zone, this expansion induces a stress transfer from subfaults to the surrounding rock matrix, with increased stresses and strains propagating to the core. Consequently, an increase in compressive stress is observed near the core where fluid diffusion in the damaged matrix is blocked on one side by the low-permeable core and on the other side by the low-porosity protolith. This poroelastic stressing causes an increase in total normal and shear stress in the core (Figures 3e and 3f), which induces a contraction ($\Delta\varepsilon = 2.25\%$) and a vertical slip of about 12 m (Figures 3c and 3g). This slip is distributed along a 175 m long active shear zone (Figure 3g) when the damage zone is simulated, whereas slip and shear zone length are lower (by a factor of $\sim$2) outside the damage zone. In both cases, fault slip occurs progressively—it could possibly be associated with an aseismic event. Models demonstrate that poroelastic effects occurring in the damage zone have a significant impact on the resulting hydromechanical fault core behavior, by driving fluid and stress transfer.

5. Conclusion

[18] Our in situ investigations at Coaraze indicated the significant role of coupled stress, strain, and pore-fluid diffusion from the damage zone to the fault core of a crustal strike-slip fault zone, during a spontaneous pressurization. The hydromechanical behavior of the damage zone is interpreted as a stress transfer and—extended through numerical simulations to seismogenic depths—may play a central role in the nucleation of earthquake ruptures. This is because, stress transfer controls the evolution of rock/fluid parameters, as well as how the static poroelastic stress transfer can be accumulated near the creeping fault core in inter-seismic periods and during slow aseismic slip events—as has been reported in several subduction zones [*Rogers and Dragert*, 2003]. Our results thus suggest that the structural evolution of faults may be linked with the hydromechanical properties of the surrounding zones, highlighting the relationship between hydraulic diffusivity and stress transfer.

References

Caine, J. S., J. P. Evans, and C. G. Foster (1996), Fault zone architecture and permeability structures, *Geology*, *24*(11), 1025–1028.

Cappa, F., Y. Guglielmi, P. Fénart, V. Merrien, and A. Thoraval (2005), Hydromechanical interactions in a fractured carbonate reservoir inferred from hydraulic and mechanical measurements, *Int. J. Rock Mech. Min. Sci.*, *42*, 287–306.

Davies, J. P., and D. K. Davies (1999), Stress-dependent permeability: Characterization and modeling, SPE paper 56813 presented at the SPE Annual Technical Conference and Exhibition, Houston, Tex., 3–6 Oct.

Gudmundsson, A. (1999), Fluid overpressure and stress drop in fault zones, *Geophys. Res. Lett.*, *26*(1), 115–118.

Gudmundsson, A. (2000), Active fault zones and groundwater flow, *Geophys. Res. Lett.*, *27*(18), 2993–2996.

Gudmundsson, A. (2004), Effects of Young's modulus on fault displacement, *C. R. Geosci.*, *336*, 85–92.

Gudmundsson, A., S. S. Berg, K. B. Lyslo, and E. Skurtveit (2001), Fracture networks and fluid transport in active fault zones, *J. Struct. Geol.*, *23*, 343–353.

Guglielmi, Y. (1998), Hydromechanics of fractured rock masses: Results from an experimental site in limestone, in *Mechanics of Jointed and Faulted Rock*, edited by H.-P. Rossmanith, pp. 621–624, A. A. Balkema, Brookfield, Vt.

Husen, S., E. Kissling, and E. R. Flueh (2000), Local earthquake tomography of shallow subduction in north Chile: A combined onshore and offshore study, *J. Geophys. Res.*, *105*(B12), 28,183–28,198.

Larroque, C., N. Bethoux, E. Calais, F. Courboulex, A. Deschamps, J. Deverchère, J. F. Stéphan, J. F. Ritz, and E. Gilli (2001), Active and recent deformation at the Southern Alps-Ligurian basin junction, *Neth. J. Geosci.*, *80*(3–4), 255–272.

Miller, S. A., C. Collettini, L. Chiaraluce, M. Cocco, M. Barchi, and B. J. P. Kaus (2004), Aftershocks driven by a high-pressure CO_2 source at depth, *Nature*, *427*, 724–727.

Rogers, G., and H. Dragert (2003), Episodic tremor and slip on the Cascadia subduction zone: The chatter of silent slip, *Science*, *300*, 1942–1943.

Sibson, R. H., and J. V. Rowland (2003), Stress, fluid pressure and structural permeability in seismogenic crust, North Island, New Zealand, *Geophys. J. Int.*, *154*, 584–594.

Uehara, S. I., and T. Shimamoto (2004), Gas permeability evolution of cataclasite and fault gouge in triaxial compression and implications for changes in fault-zone permeability structure through the earthquake cycle, *Tectonophysics*, *378*, 183–195.

Wibberley, C. A. J., and T. Shimamoto (2003), Internal structure and permeability of major strike-slip fault zones: The Median Tectonic Line in Mie Prefecture, southwest Japan, *J. Struct. Geol.*, *25*, 59–78.

Zhao, D., H. Kanamori, H. Negishi, and D. Wiens (1996), Tomography of the source area of the 1995 Kobe earthquake: Evidence for fluids at the hypocenter?, *Science*, *274*, 1891–1894.

F. Cappa, Earth Sciences Division, Lawrence Berkeley National Laboratory, Berkeley, CA 94720, USA. (fcappa@lbl.gov)

Y. Guglielmi and J. Virieux, Géosciences Azur, CNRS-UNSA-IRD-UPMC, F-06560 Sophia Antipolis, France. (gugliemi@geoazur.unice.fr; virieux@geoazur.unice.fr)